# Stress State of the Earth Dam Taking into Account Water Pressure and Moisture of Soil

Sadillakhon Umarkhonov[1,a)]

[1]*Institute of Mechanics and Seismic Stability of Structures named after M.T. Urazbaev, Uzbekistan Academy of Sciences, Tashkent, Uzbekistan*

[a)]Corresponding author: umarkhonov@gmail.com

**Abstract.** Globally, earth dams represent the most frequent type of dam construction. Their reliance on readily available, native materials results in a much lower cost compared to concrete dams. Ensuring the structural integrity of earth dams is of utmost importance in seismic areas. Every earth dam is characterized by its own specific design parameters and geographical setting. Essential for the Tashkent region's inhabitants, the Akhangaran Dam is instrumental in delivering drinking water and generating electricity. The present article is dedicated to the dynamic analysis of the stress-strain response of earth dams when subjected to seismic loads. To understand the behavior of earth dams, the study uses a developed method for solving wave equations to determine their stress-strain conditions. An algorithm is developed using the finite difference method. This algorithm is designed to solve problems and employs computational formulas that achieve second-order accuracy in both temporal and spatial dimensions. This method excels because it can handle intricate, non-linear models. These models can accurately represent how a structure changes and how soil conditions, like moisture content, fluctuate. The behavior of an earth dam during an earthquake is the subject of a numerical study. Through this research, the stress-strain state of the dam is quantified, and the temporal change of stresses, strains, and displacements at defined locations is tracked.

## INTRODUCTION

The significant threat of catastrophic events from earth dam malfunctions drives a greater need for their dependable operation, which is then translated into the relevant design standards. The operational characteristics of earth dams situated on natural foundations are not yet thoroughly investigated. Investigations into the strength, deformation, and stability of earth dams have been carried out by many scientists, considering the effects of static and dynamic forces [1-10]. Predicting stress and strain variations in earth dams caused by loads such as soil weight, water pressure, and seismic events requires knowledge of the soil's deformability and strength characteristics. The physical and mechanical properties of the soil within the dam body and its foundation influences to distribution of stress and strain is significantly, considering the structure's geometric properties, along with variations in reservoir water levels, seismic activity, and other influences. The stress and strain within dams are evaluated using numerical simulations. The structural integrity of an earthen dam must be proven by demonstrating its ability to withstand conditions that would lead to catastrophic failure. An analysis of the earth dam's stress-strain behavior will provide the necessary stress and strain values The paper's purpose is to outline a method for studying the dynamic response of earth dams, based on principles of the mechanics of deformable rigid bodies.

## PROBLEM STATEMENT AND SOLUTION

We are looking at earth dams that are built on a rigid foundation. (Fig. 1). In cases where the dam's length is substantially greater than its width and height, its dynamic behavior can be considered as a plane-strain problem. If seismic load forces act on the base of an earth dam (Fig. 2), movement commences inside the dam's substance. The earth dam's equation of motion is:

$$\rho \frac{d\upsilon_x}{dt} = \frac{\partial S_{xx}}{\partial x} + \frac{\partial P}{\partial x} + \frac{\partial \tau_{xy}}{\partial y}, \quad \rho \frac{d\upsilon_y}{dt} = \frac{\partial S_{yy}}{\partial y} + \frac{\partial P}{\partial y} + \frac{\partial \tau_{xy}}{\partial x} - \rho g. \tag{1}$$

This describes the movement of particles, where $\upsilon_x$ represents their speed in the horizontal direction (x-axis) and $\upsilon_y$ represents their speed in the vertical direction (y-axis). $S_{xx}$, $S_{yy}$, *and* $\tau_{xy}$ represent the deviatoric stress components; $\rho$ is the density; $P$ is the pressure.

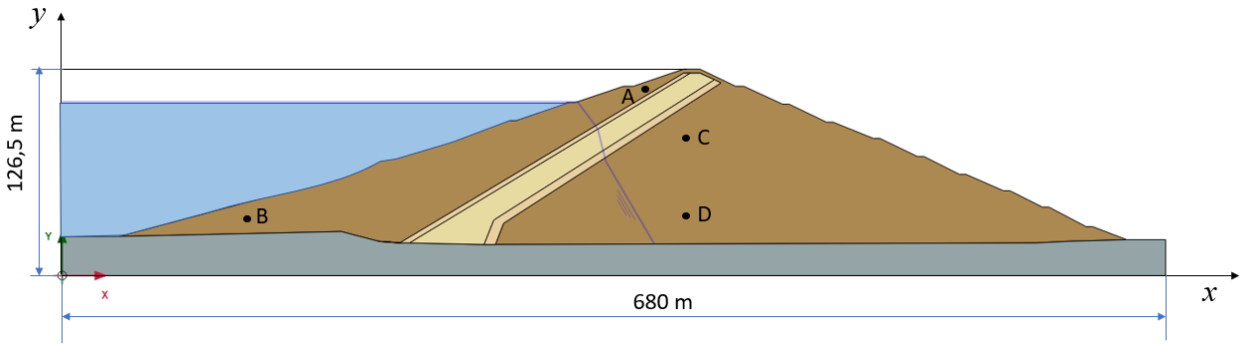


**FIGURE 1**. A cross cutaway of earth dam

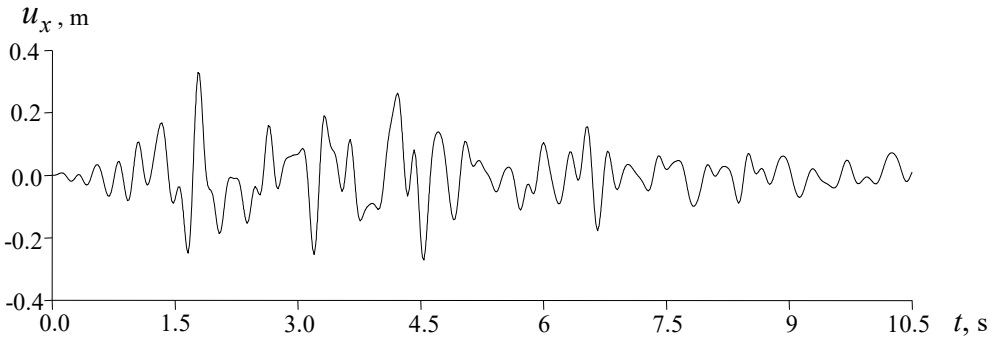


**FIGURE 2.** Seismological velocity recordings obtained at the Akhangaran Dam's toe during the earthquake

The total stresses are given by the following equations:

$$\sigma_{xx} = S_{xx} + \mathrm{P}, \quad \sigma_{yy} = S_{yy} + \mathrm{P}, \quad \sigma_{zz} = S_{zz} + \mathrm{P}. \tag{2}$$

Earth dam deformation is modeled with nonlinear equations:

$$\dot{P} = -\left(\lambda + \frac{2}{3}\mu\right)\frac{\dot{V}}{V}, \tag{3}$$

$$\frac{dS_{xx}}{dt} + \lambda S_{xx} = 2G\left(\frac{d\varepsilon_{xx}}{dt} - \frac{dV}{3Vdt}\right), \quad \frac{dS_{yy}}{dt} + \lambda S_{yy} = 2G\left(\frac{d\varepsilon_{yy}}{dt} - \frac{dV}{3Vdt}\right), \tag{4}$$

$$\frac{dS_{zz}}{dt} + \lambda S_{zz} = 2G\left(\frac{d\varepsilon_{zz}}{dt} - \frac{dV}{3Vdt}\right), \quad \frac{d\tau_{xy}}{dt} + \lambda \tau_{xy} = 2G\frac{d\tau_{xy}}{dt}. \tag{5}$$

The relationship between ultimate strength and pressure, as described by the generalized von Mises condition, is expressed as follows:

$$S_{xx}^2 + S_{yy}^2 + S_{zz}^2 + 2\tau_{xy}^2 \le \frac{2}{3}[Y(P)]^2 \tag{6}$$

$$Y(P) = Y_0 + \frac{\mu P}{1 + \mu P/(Y_{PL} - Y_0)}, \tag{7}$$

$K$ and $G$ - the bulk compression and shear moduli: $V=\rho_0/\rho$ - relative volume; $Y_0$ - cohesion; $\mu$ - friction coefficient; $Y_{PL}$ - the ultimate shear strength of the rock fill; $\lambda$ - the functional defined by the following equations:

$$\lambda = \frac{3W}{2Y^2} H(W), \quad H(W) = \begin{cases} 1, & \text{at } W \geq 0 \\ 0, & \text{at } W < 0 \end{cases}, \quad W = 2\mu \left\{ \sum_{j=x,y,z} S_{jj} \left( \frac{d\varepsilon_{jj}}{dt} - \frac{1}{3} \frac{dV}{Vdt} \right) + \tau_{xy} \frac{d\varepsilon_{xy}}{dt} \right\}. \tag{8}$$

The equations (1) through (7) need to be add with equations that connect the strain rate components to the mass velocities. The equation describing soil continuity is:

$$\frac{d\varepsilon_{xx}}{dt} = \frac{\partial U_x}{\partial x}, \quad \frac{d\varepsilon_{yy}}{dt} = \frac{\partial U_y}{\partial y}, \quad \frac{d\varepsilon_{xy}}{dt} = \frac{1}{2} \left( \frac{\partial U_y}{\partial x} + \frac{\partial U_x}{\partial y} \right). \tag{9}$$

$$. \frac{dV}{dt} - V \cdot \left( \frac{\partial U_x}{\partial x} + \frac{\partial U_y}{\partial y} \right) = 0 \ . \tag{10}$$

The mechanical parameters of the soil are to be considered as functions of moisture content, formulated as:

$$K(I_W) = K_{sat} \exp(\alpha_K (1 - I_W)) \tag{11}$$

$$G(I_W) = G_{sat} \exp(\alpha_G (1 - I_W)) \tag{12}$$

$$c(I_W) = c_{sat} \exp(\beta(1 - I_W)) \tag{13}$$

$$\mu(I_W) = \mu_{sat} \exp(\gamma(1 - I_W)) \qquad I_W = W/W_{sat} \tag{14}$$

$$Y(P, I_W) = c(I_W) + \mu(I_W) \cdot P \tag{15}$$

Here, $K_{sat}$ represents the bulk modulus, $G_{sat}$ denotes the shear modulus, $c_{sat}$ signifies the cohesion, and $\mu_{sat}$ - is the coefficient related to the angle of internal friction from fully saturated soil. The extent of soil moisture content is indicated by $I_W$. $W$ is the current moisture level, and $W_{sat}$ is the moisture content at full saturation.

Consequently, the set of differential equations, numbered (1) through (15), forms a complete system. When supplemented with initial and boundary conditions, it accurately describes the the stress-strain characteristics of an earth dam. The dam's surface is stress-free. Initial conditions are set to zero.

The earth dam is characterized by the following measurements: It stands 110 meters tall. The top of the dam is 10 meters wide, while the base spans 680 meters. The sides slope at a rate of 1:2 on the upper portion and 1:1.9 on the lower portion. A central core within the dam has widths of 110 meters and 12 meters. The following physical and mechanical parameters of the earth dam were taken: for the slope: the density - 2100 kg/m$^3$, the modulus of elasticity -$E_{dam}$=4000 MPa, the Poisson's ratio - $\nu_{dam}$=0.3. The slope strength indicators (cohesion, friction coefficient, ultimate shear strength) were $Y0=\mu/800$, $\mu$=0.4, $Y_{dam}=20Y_0$ . For the core: the density - 1780 kg/m$^3$; the modulus of elasticity - $E_{core}$=2000 MPa; the Poisson's ratio - $\nu_{core}$=0.3. The slope strength indicators (cohesion, friction coefficient, ultimate shear strength) were $Y_0=\mu/1000$, $\mu$=0.3, $Y_{core}=20Y_0$.

## RESULTS

Numerical solutions for the dynamic problems will be obtained using the finite difference method, specifically the quadrilateral mesh scheme of M.Wilkins. In non-stationary problems, In dynamic scenarios, time (t) plays a significant role as an independent variable. Discretizing this variable means calculations occur in discrete time steps, each representing the state change from $t_0$ to $t_0 + \Delta t$. Wilkins' scheme's advantage lies in its self-adjusting time step (Δt), which is determined by stability and accuracy needs during computation.

The static problem was solved using Plaxis 2D, a finite element method program, considering water pressure and the earth dam's moisture content.

Seismic forces were employed to represent dynamic forces. Seismic loading at the foundation of an earth dam generates particle movement and soil deformation within the dam.

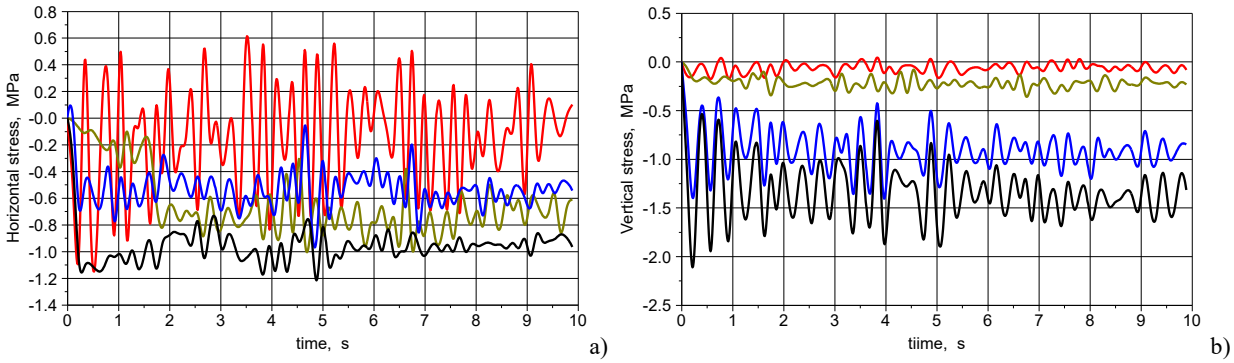


a) b)

The red line is point A, the green line is point B, the blue line is point C, and the black line is point D.

**FIGURE 3.** Change in horizontal (a) and vertical (b) stresses by time

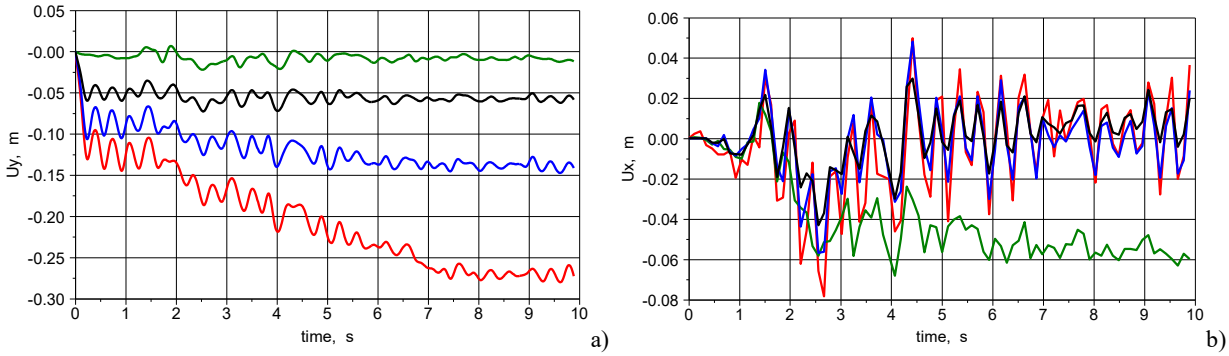


a) b)

The red line is point A, the green line is point B, the blue line is point C, and the black line is point D.

**FIGURE 4.** Change in horizontal (a) and vertical (b) displacement by time

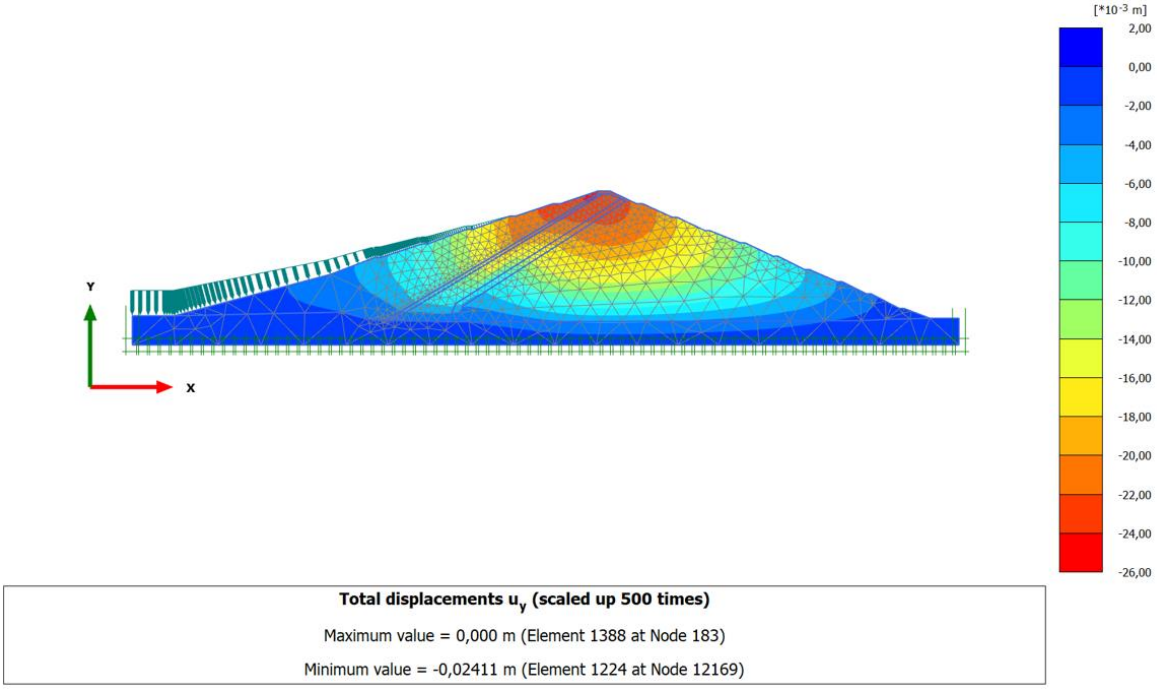


**FIGURE 5.** Vertical displacements on the of the dam

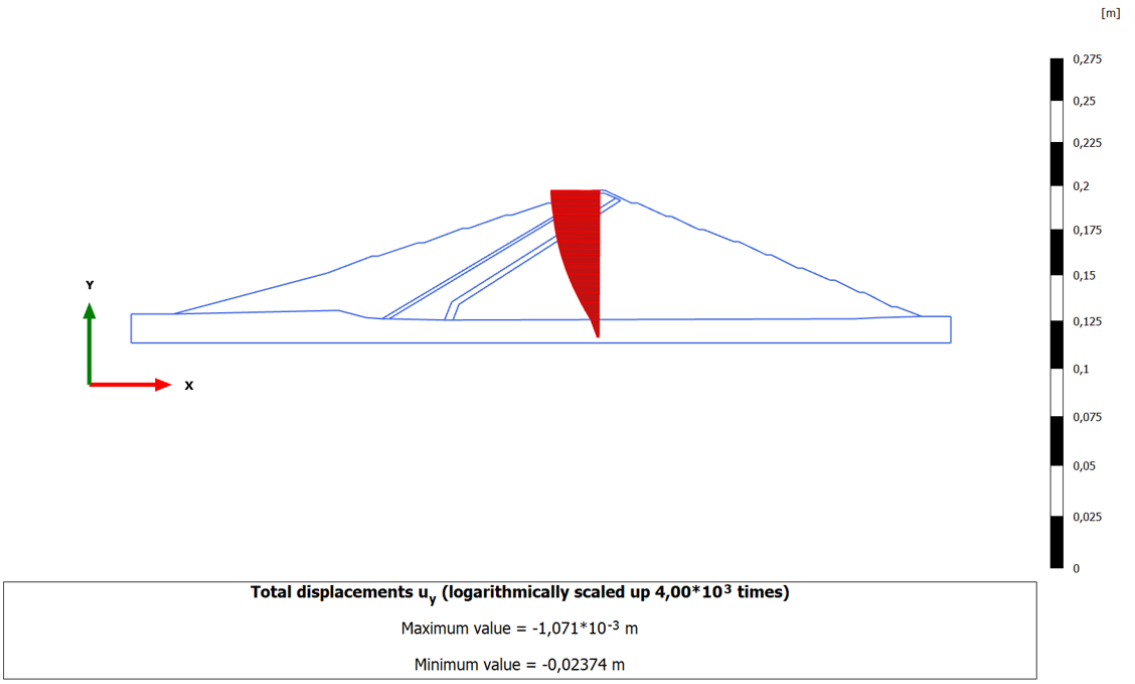


**FIGURE 6.** Vertical displacement diagram in the middle of an earth dam

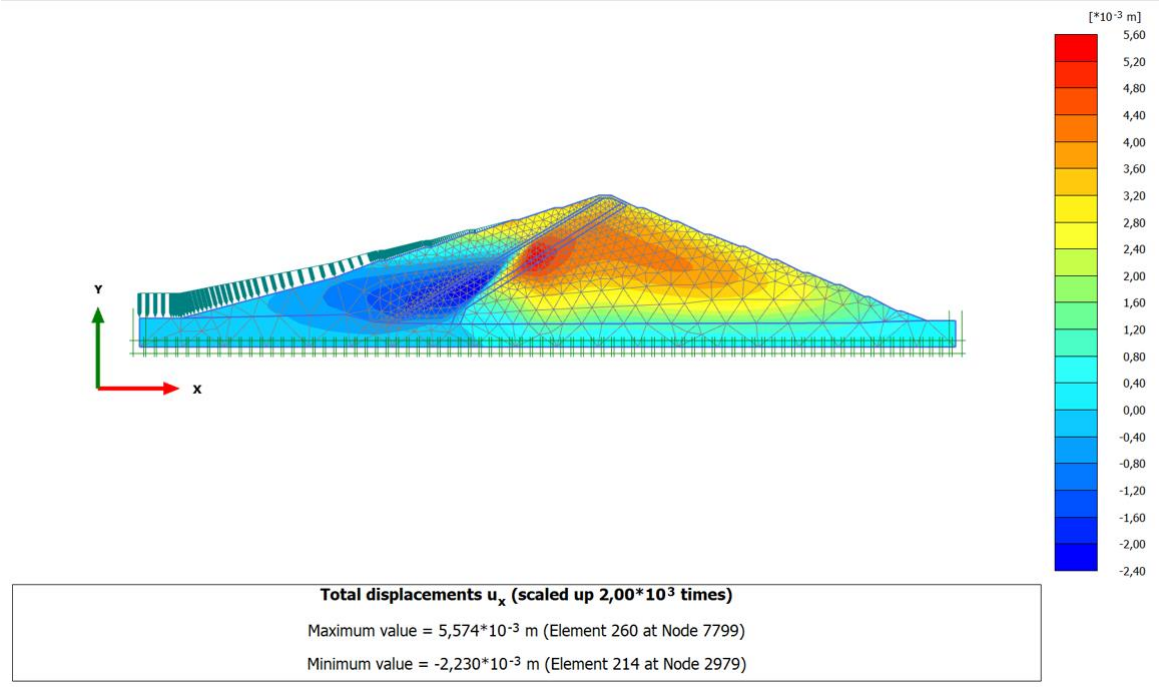


**FIGURE 7.** Horizontal displacements of the dam

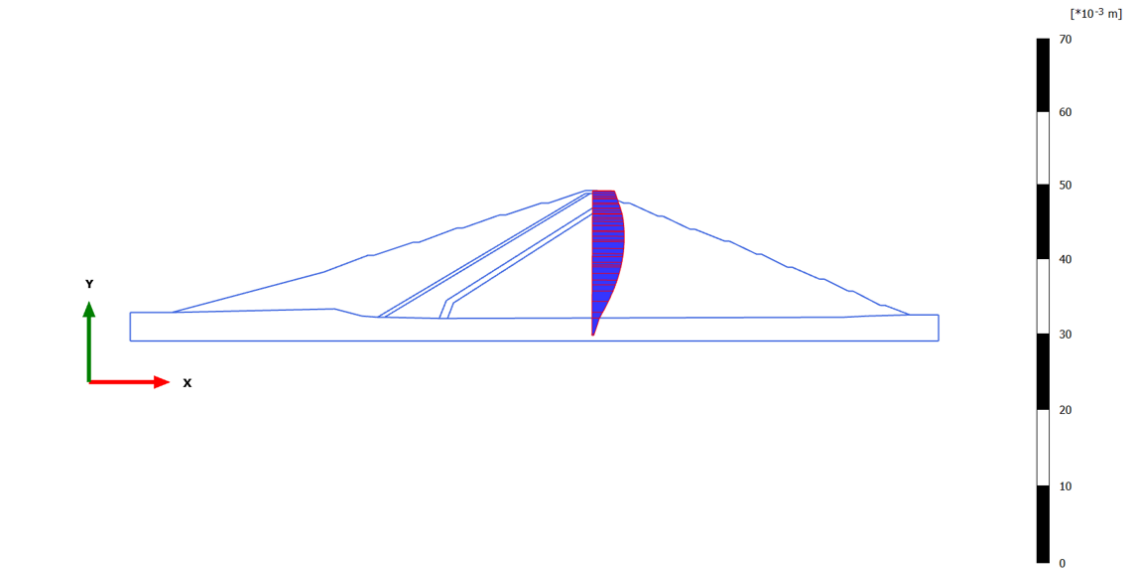


**FIGURE 8.** Horizontal displacement diagram at the middle of an earth dam

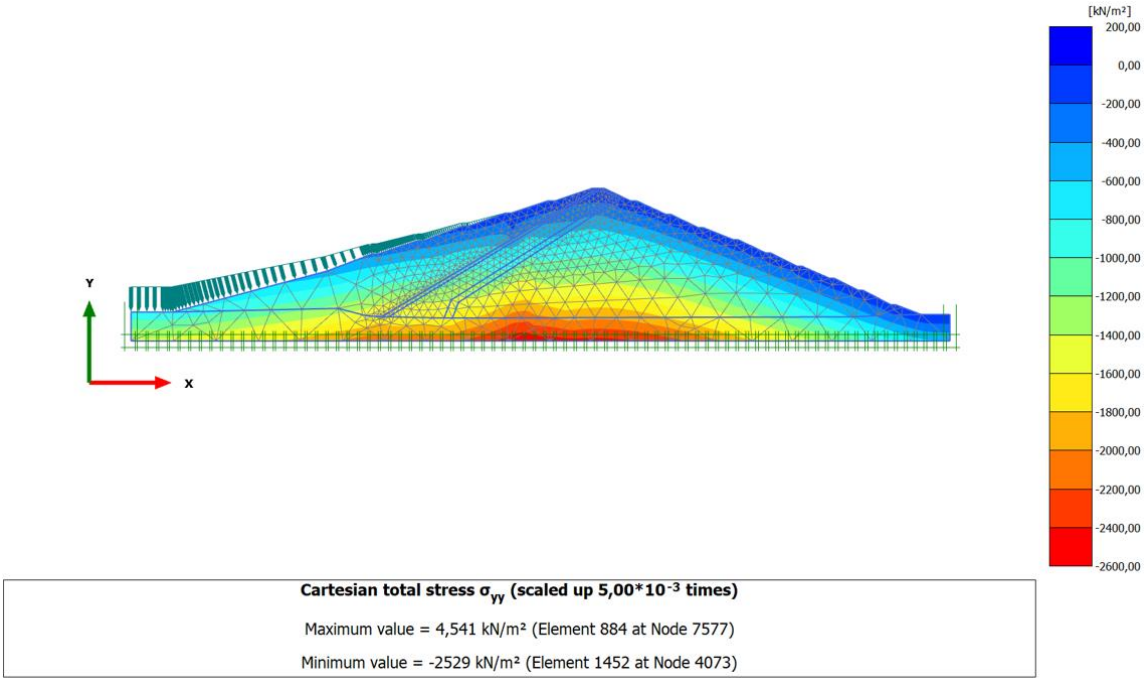


**FIGURE 9.** Vertical stresses of the dam

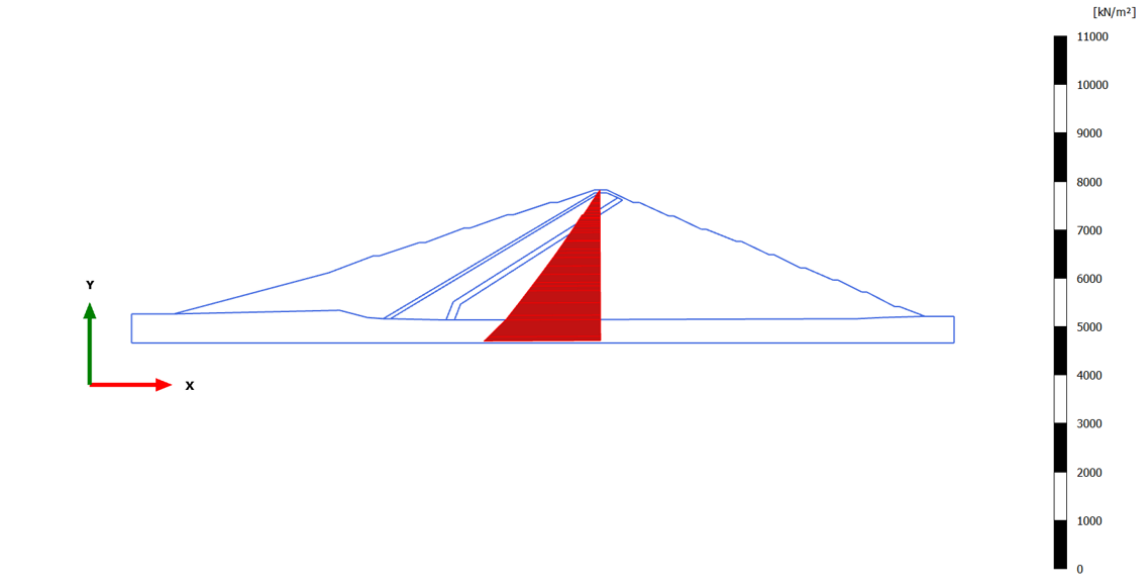


**Cartesian total stress $\sigma_{yy}$ (scaled up 0,0400 times)**

Maximum value = -0,1270 kN/m²

Minimum value = -2418 kN/m²

**FIGURE 10.** Vertical stress diagram at the middle of an earth dam

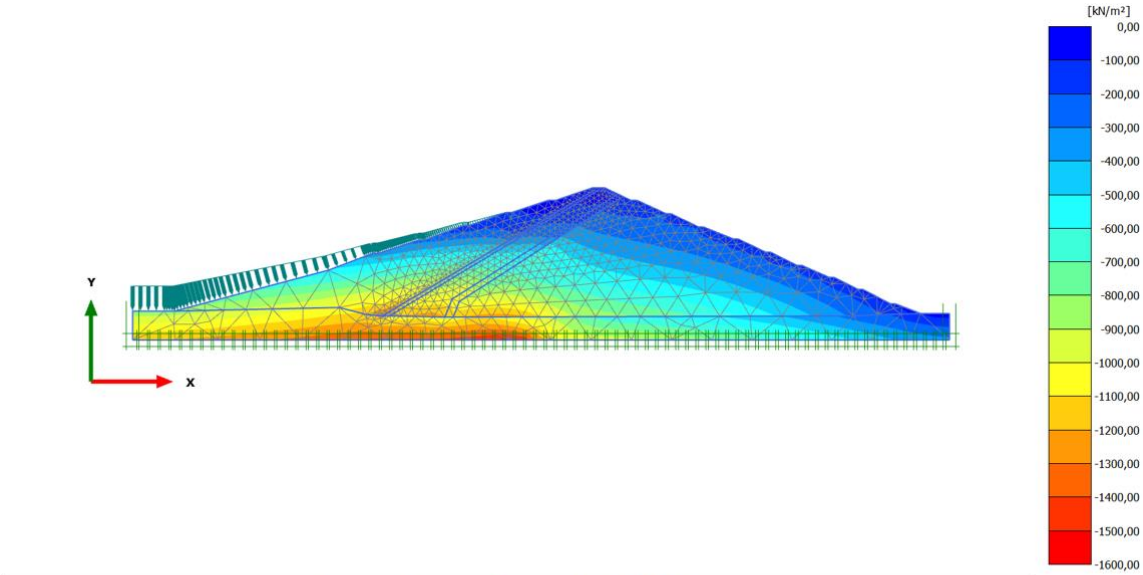


**Cartesian total stress $\sigma_{xx}$ (scaled up 0,0100 times)**

Maximum value = -10,32 kN/m² (Element 703 at Node 11405)

Minimum value = -1538 kN/m² (Element 1393 at Node 4071)

**FIGURE 11.** Horizontal stresses of the dam

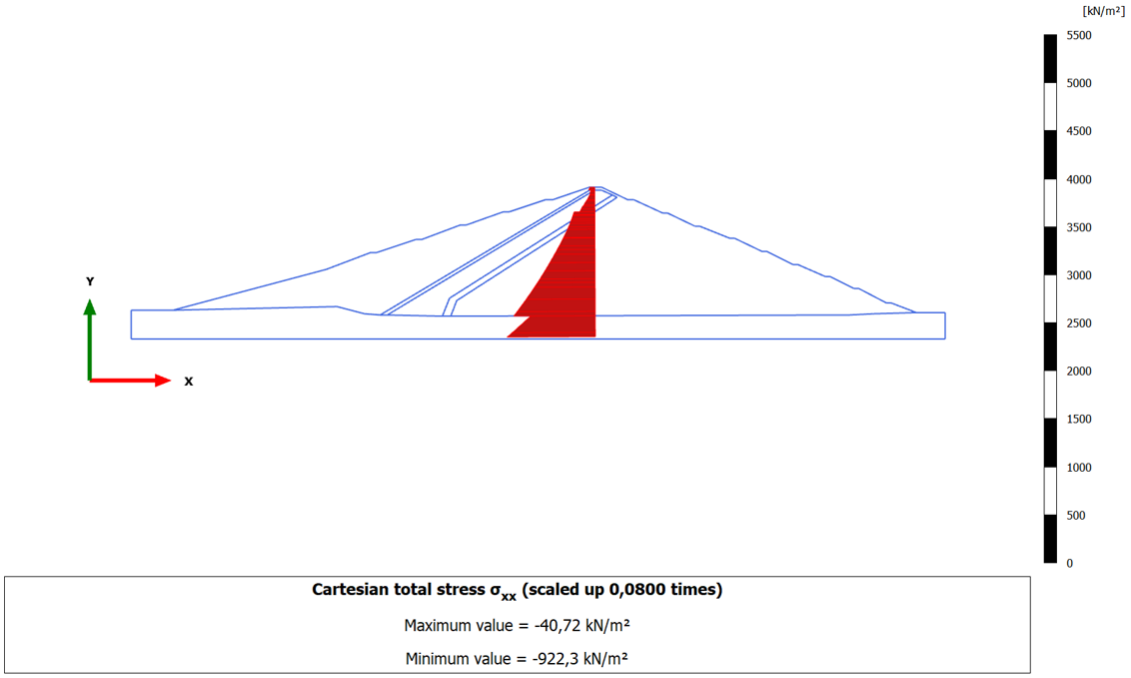


**FIGURE 12.** Horizontal stress diagram at the middle of an earth dam

## ANALYSIS OF RESULTS

Changes in horizontal and vertical stresses over time in an earth dam's cross-section, due to seismic forces, are shown in Figure 3. The blue, green, black, and red curves in this figure denote stress changes at points A, B, C, and D, respectively. The figures lead us to the conclusion that the greatest horizontal and vertical stresses are found at the lowest point D. The highest horizontal stress is -1.2 MPa, and the highest vertical stress is -2.2 MPa. Changes in horizontal and vertical displacement over time in an earth dam's cross-section are shown in Figure 4. The maximum value of the vertical displacement occurs in the upper part of the dam, i.e., at point A.

Figure 5 shows the pattern of vertical displacement across the earth dam's cross-section. The most significant downward vertical displacement, -0.024 m, is found at the top of the dam. Figure 6 details the vertical displacements within the dam's central axis, revealing no settlement at the foundation while the upper section experiences the greatest displacement. Figure 7 presents the contour lines for horizontal displacements across the earth dam's cross-section, with the largest recorded horizontal shift being 0.005 m. This figure also illustrates the horizontal displacement profile along the dam's center, indicating a rightward displacement caused by water pressure from the left. Within the dam's center, horizontal displacement escalates from the base upwards, beginning at zero at the bottom and reaching its peak at the very top. Figure 8 provides a graphical representation of vertical displacements along the dam's central axis. The depicted figure demonstrates that the maximum value of vertical stress is situated in the central lower region of the dam. The stress values along the slope above the water level and the right slope are zero. In Figure 10, the representation of vertical stresses within the mid-section of the earth dam indicates that the maximum value of vertical stress is -2.41 MPa. Figure 11 presents the isolines of horizontal stresses within the cross-section of the earth dam. Subsequently, Figure 12 illustrates the diagram of horizontal stresses in the middle of the earth dam. From this analysis, it can be deduced that the maximum value of horizontal stress is -0.92 MPa is recorded at the bottom

## CONCLUSION

The stress-strain behavior of the Akhangaran earth dam under seismic excitation was determined, factoring in moisture content, water pressure, and the dam's weight.

Changes in horizontal and vertical stresses were observed and analyzed at significant points of the dam when subjected to seismic load.

A static and dynamic analysis were performed on the earth dam, generating isolines and diagrams that map displacement and stress components, while considering the effects of material moisture content and hydrostatic pressure.

Analysis of the generated graphs, which account for water pressure, indicates that the greatest vertical displacements occurred at the top of the dam, with vertical stresses reaching -0.27 m and horizontal stresses measuring 0.08 m.

## ACKNOWLEDGMENTS

This investigation was provided by the budgetary funding of the Institute of Mechanics and Seismic Stability of Structures named after M.T.Urazbaev, Uzbekistan Academy of Sciences. We extend our deepest gratitude to the Academy for its unwavering support and dedication to advancing scientific research.

## REFERENCES

1. S. P. Bakhaeva and D. V. Gur'ev**,** Stability prediction in earthfill dams with regard to spatial variability of strength properties of loamy soil, *J. Min. Sci.* **56**(1), 88–96 (2020), https://doi.org/10.1134/S1062739120016442.
2. M. M. Mirsaidov, T. Z. Sultanov, and A. Sadullaev**,** Determination of the stress-strain state of earth dams with account of elastic-plastic and moist properties of soil and large strains, *Mag. Civ. Eng.* **40**, 59–68 (2013), https://doi.org/10.5862/MCE.40.7.
3. K. Sultanov, S. Umarkhonov, and S. Normatov**,** Calculation of earth dam strain under seismic impacts, in *International Conference on Actual Problems of Applied Mechanics – APAM-2021*, *AIP Conf. Proc.* **2637** (AIP Publishing, Melville, NY, 2022), pp. 030008, https://doi.org/10.1063/5.0118430.
4. J. Amnyattalab and H. Rezaie**,** Study of the effect of seepage through the body of earth dam on its stability by predicting the affecting hydraulic factors using models of Brooks–Corey and van Genuchten (Case study of Nazluchay and Shahrchay earth dams), *Int. J. Environ. Sci. Technol.* **15**(12), 2633–2644 (2018), https://doi.org/10.1007/s13762-017-1549-y.
5. J.-W. Seo, D.-W. Park, and T. H. M. Le**,** Development of an asphalt concrete mixture for asphalt core rockfill dam, *Constr. Build. Mater.* **140**, 301–309 (2017), https://doi.org/10.1016/j.conbuildmat.2017.02.100.
6. E. Suryo, Y. Zaika, and D. Setyowulan**,** Stability analysis of earth dam slopes subjected to earthquake using ERT results interpretation, *Int. J. Civ. Eng. Technol.* **9**(11), 150–158 (2018), https://doi.org/10.21776/ub.rekayasasipil/2017.011.02.10.
7. M. Rashidi and S. M. Haeri**,** Evaluation of behaviors of earth and rockfill dams during construction and initial impounding using instrumentation data and numerical modeling, *J. Rock Mech. Geotech. Eng.* **9**(4), 709–725 (2017), https://doi.org/10.1016/j.jrmge.2016.12.003.
8. T. Li, M. Motagh, M. Wang, W. Zhang, C. Gong, X. Xiong, J. He, L. Chen, and J. Liu**,** Earth and rock-filled dam monitoring by high-resolution X-band interferometry: Gongming dam case study, *Remote Sens.* **11**(3), 246 (2019), https://doi.org/10.3390/rs11030246.
9. Maimunah, M. Yeni, and D. Kumala**,** Influence of water level fluctuation on the reservoir stability of an earth dam, *IOP Conf. Ser.: Mater. Sci. Eng.* **506**(1), 012032 (2019), https://doi.org/10.1088/1757-899X/506/1/012032.
10. A. Nardo, E. Cascone, G. Biondi, G. di Filippo, and O. Casablanca**,** Influence of vertical ground motion on the seismic performance of an earth dam, in *Springer Ser. Geomech. Geoeng.* (2023), https://doi.org/10.1007/978-3-031-34761-0_82